Supplement of:
Effects of Strongly Enhanced Atmospheric Methane Concentrations in a Fully Coupled Chemistry-Climate Model

Laura Stecher[1], Franziska Winterstein[1], Martin Dameris[1], Patrick Jöckel[1], Michael Ponater[1], and Markus Kunze[2]

[1]Deutsches Zentrum für Luft- und Raumfahrt (DLR), Institut für Physik der Atmosphäre, Oberpfaffenhofen, Germany
[2]Freie Universität Berlin, Berlin, Germany

Correspondence: Laura Stecher (Laura.Stecher@dlr.de)

Contents

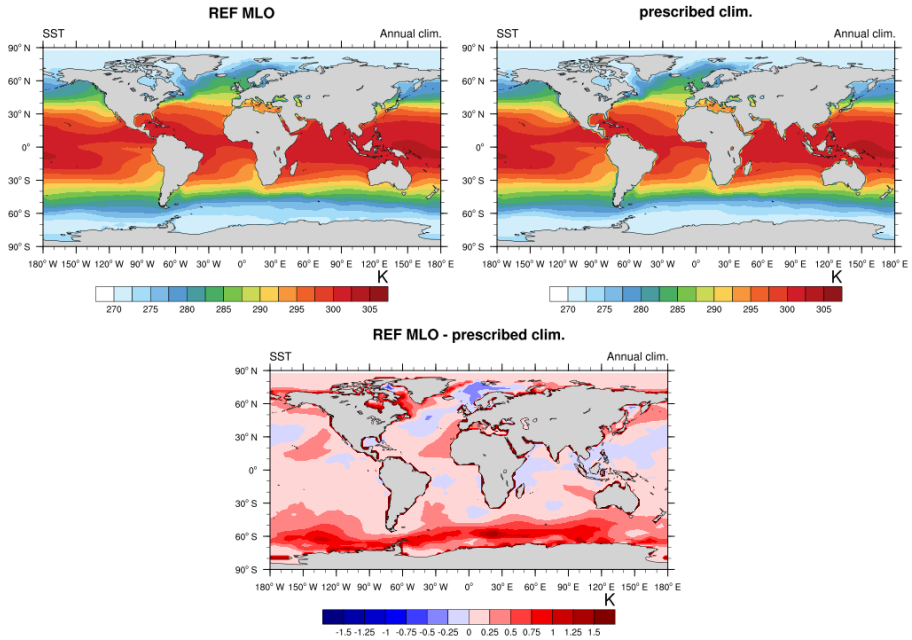

Figure S1. Climatologies of annual mean sea surface temperatures (SSTs) of REF MLO (top left) and the climatology (Rayner et al., 2003) prescribed as lower boundary for REF QFLX and REF fSST (top right), and their difference (bottom middle).

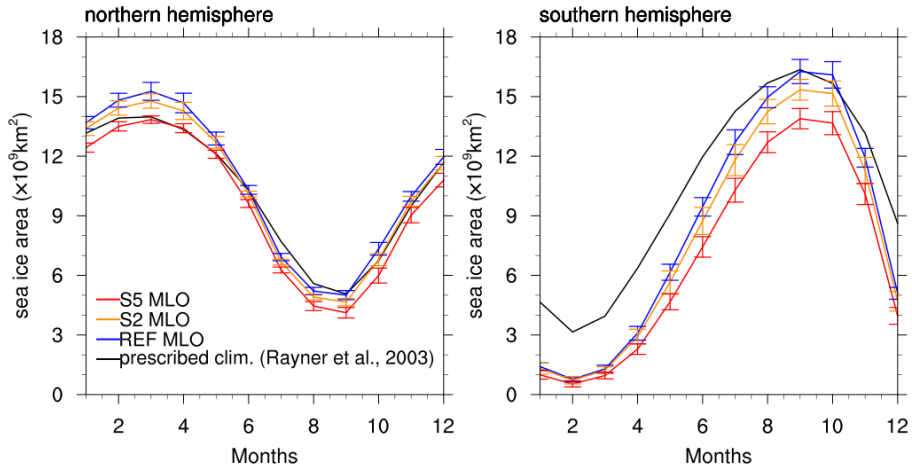

Figure S2. Monthly climatologies of total sea ice area in the Northern Hemisphere (left) and in the Southern Hemisphere (right) for REF MLO (blue), S2 MLO (orange), S5 MLO (red) and the prescribed climatology (black). For the mixed layer ocean (MLO) simulations the interannual standard deviations are indicated by vertical lines.

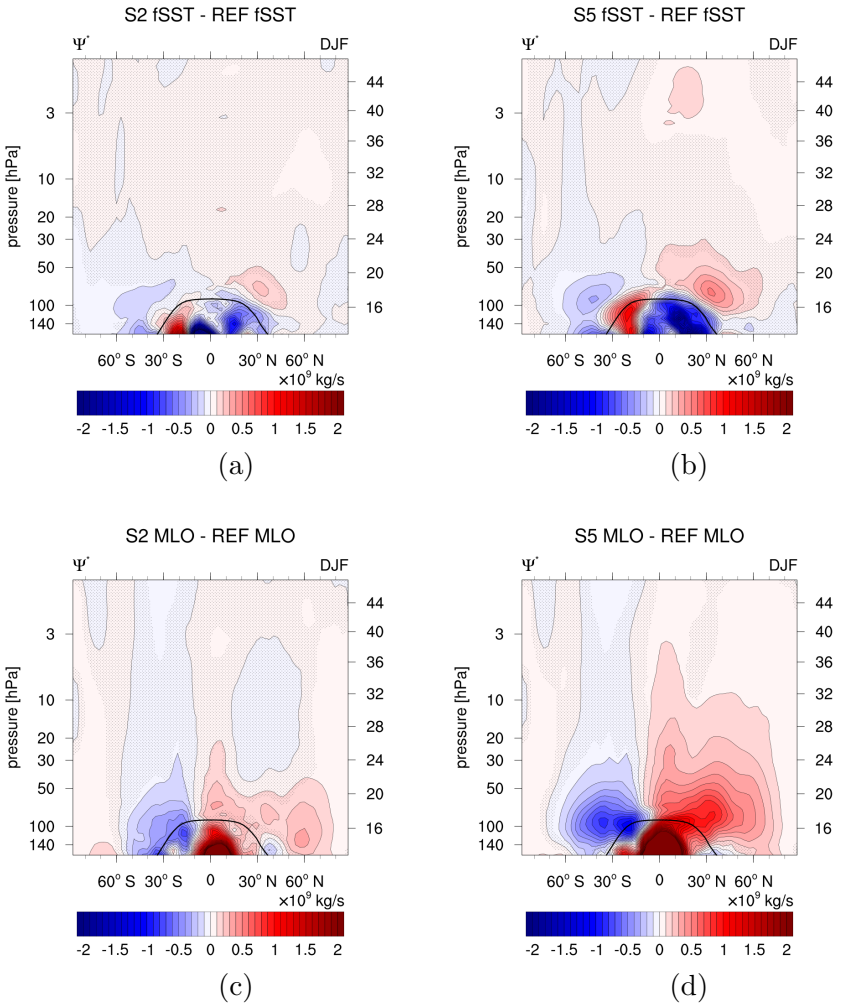

Figure S3. Absolute differences of the residual mean streamfunction for season December, January, and February (DJF) of the sensitivity simulations (a) S2 fSST, (b) S5 fSST, (c) S2 MLO, (d) S5 MLO and their respective reference in 10^9 kg s^{-1}. Non-stippled areas are significant on the 95 % confidence level according to a two sided Welch's test. The solid black line indicates the climatological tropopause height of REF MLO.

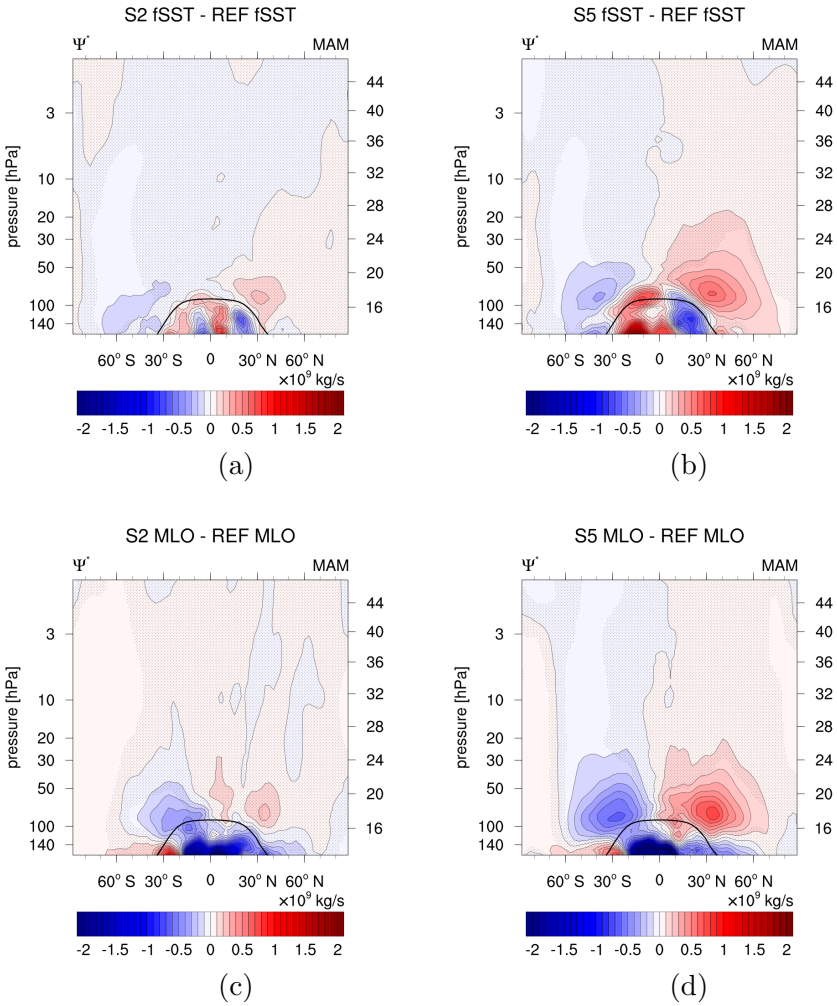

Figure S4. Absolute differences of the residual mean streamfunction for season March, April, and May (MAM) of the sensitivity simulations (a) S2 fSST, (b) S5 fSST, (c) S2 MLO, (d) S5 MLO and their respective reference in 10^9 kg s^{-1}. Non-stippled areas are significant on the 95 % confidence level according to a two sided Welch's test. The solid black line indicates the climatological tropopause height of REF MLO.

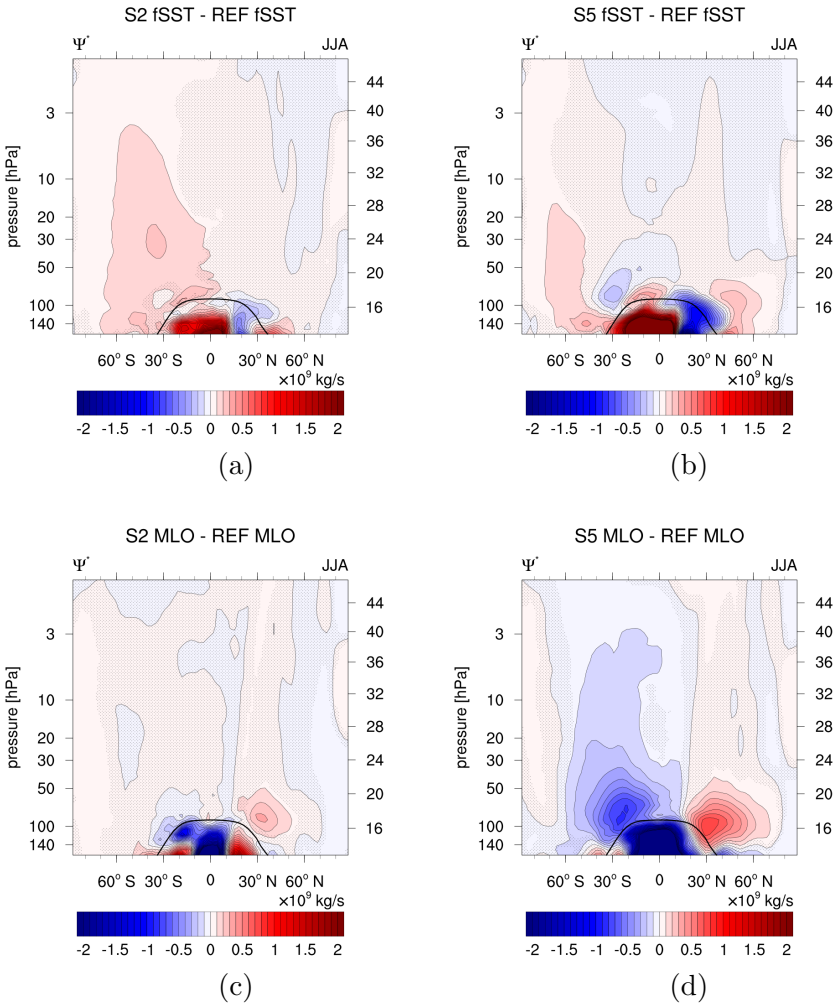

Figure S5. Absolute differences of the residual mean streamfunction for season June, July, and August (JJA) of the sensitivity simulations (a) S2 fSST, (b) S5 fSST, (c) S2 MLO, (d) S5 MLO and their respective reference in 10^9 kg s^{-1}. Non-stippled areas are significant on the 95 % confidence level according to a two sided Welch's test. The solid black line indicates the climatological tropopause height of REF MLO.

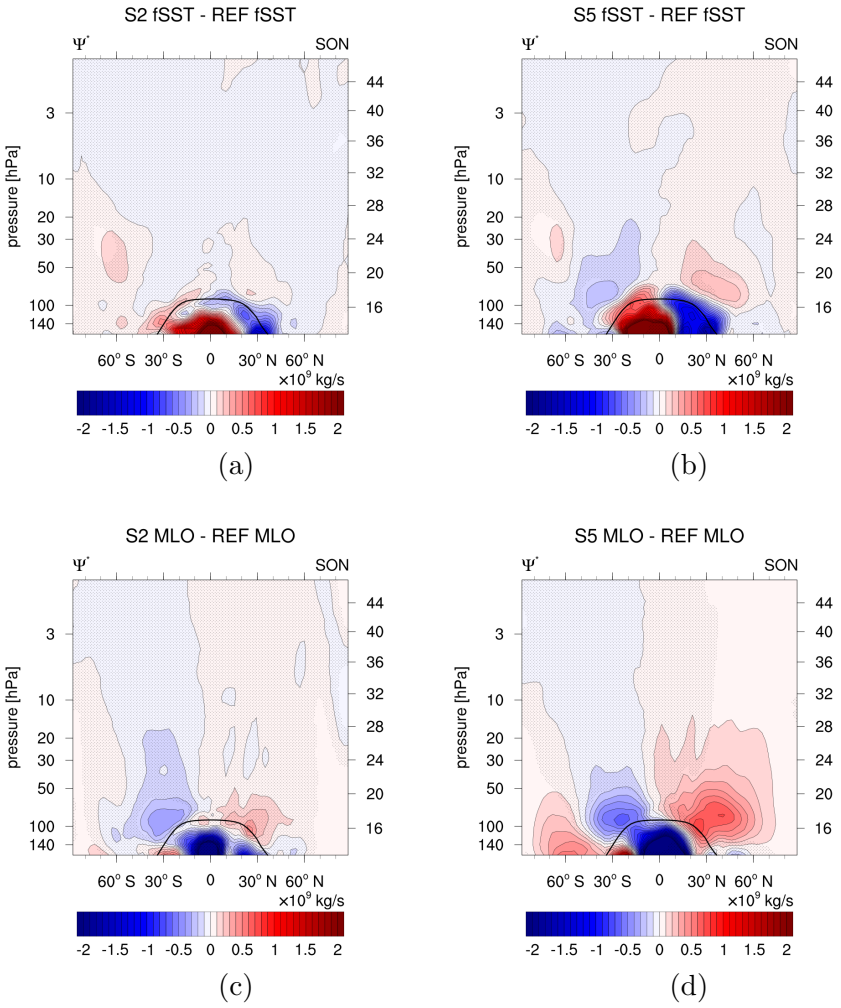

Figure S6. Absolute differences of the residual mean streamfunction for season September, October, and November (SON) of the sensitivity simulations (a) S2 fSST, (b) S5 fSST, (c) S2 MLO, (d) S5 MLO and their respective reference in 10^9 kg s^{-1}. Non-stippled areas are significant on the 95 % confidence level according to a two sided Welch's test. The solid black line indicates the climatological tropopause height of REF MLO.

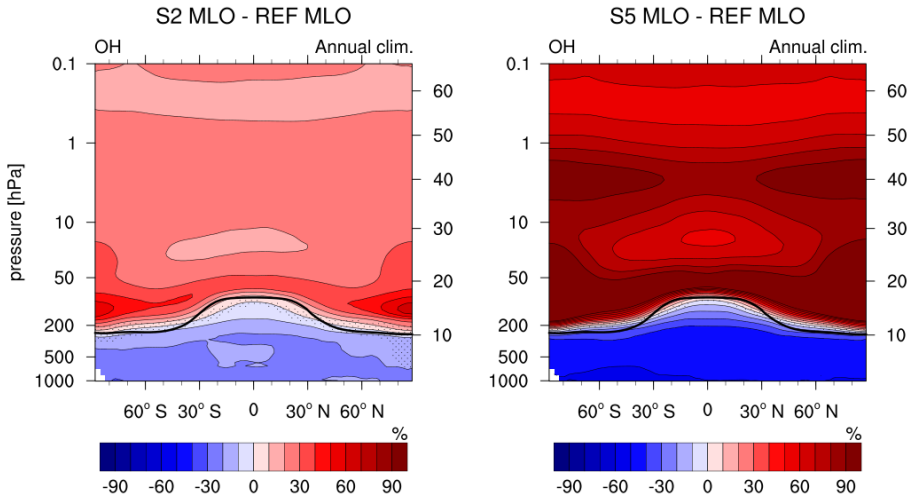

Figure S7. Relative differences between the annual zonal mean hydroxyl radical (OH) mixing ratio of the sensitivity simulations S2 MLO (left) and S5 MLO (right) and REF MLO in %. Non-stippled areas are significant on a 95 % confidence level according to a two sided Welch's test. The solid black line indicates the climatological tropopause height of REF MLO.

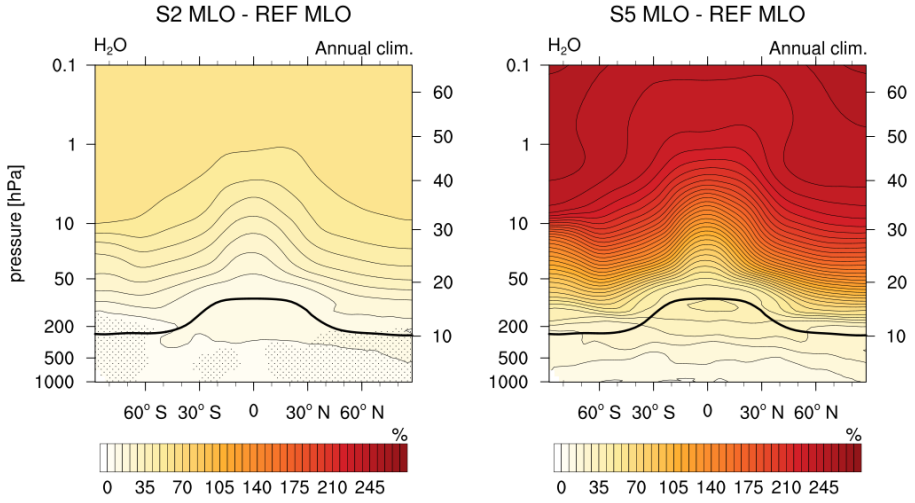

Figure S8. Relative differences between the annual zonal mean water vapour (H_2O) mixing ratio of the sensitivity simulations S2 MLO (left) and S5 MLO (right) and REF MLO in %. Non-stippled areas are significant on a 95 % confidence level according to a two sided Welch's test. The solid black line indicates the climatological tropopause height of REF MLO.

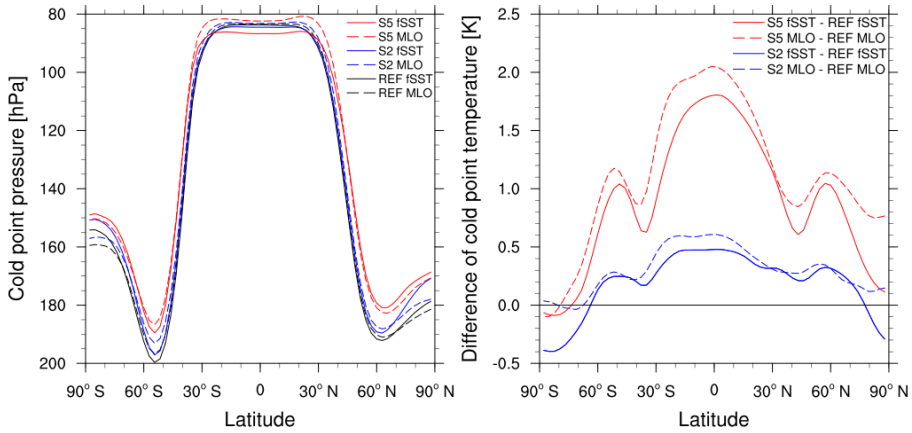

Figure S9. Cold point pressure in hPa (left) and difference of cold point temperature of the sensitivity simulations and their respective reference in K (right).

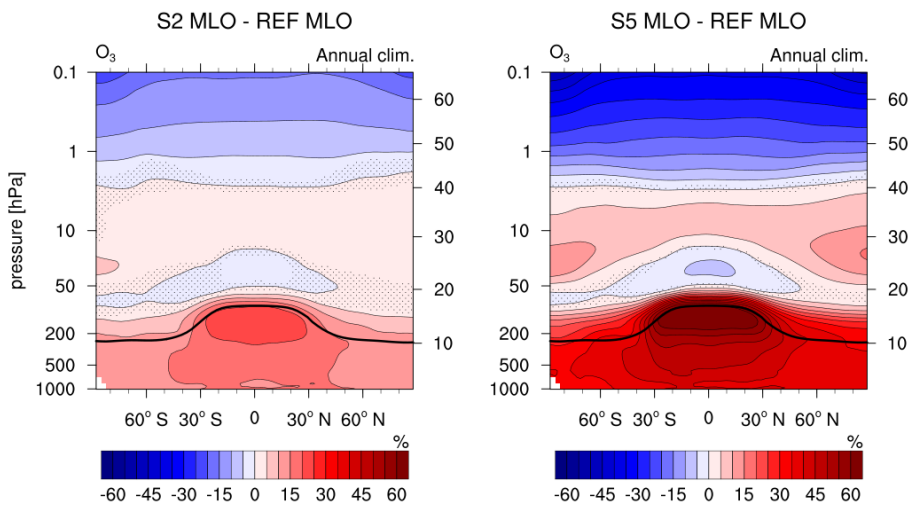

Figure S10. Relative differences between the annual zonal mean ozone (O_3) mixing ratio of the sensitivity simulations S2 MLO (left) and S5 MLO (right) and REF MLO in %. Non-stippled areas are significant on a 95 % confidence level according to a two sided Welch's test. The solid black line indicates the climatological tropopause height of REF MLO..

$\Delta T_{addst}(S2^* - REF^*)_{MLO}$

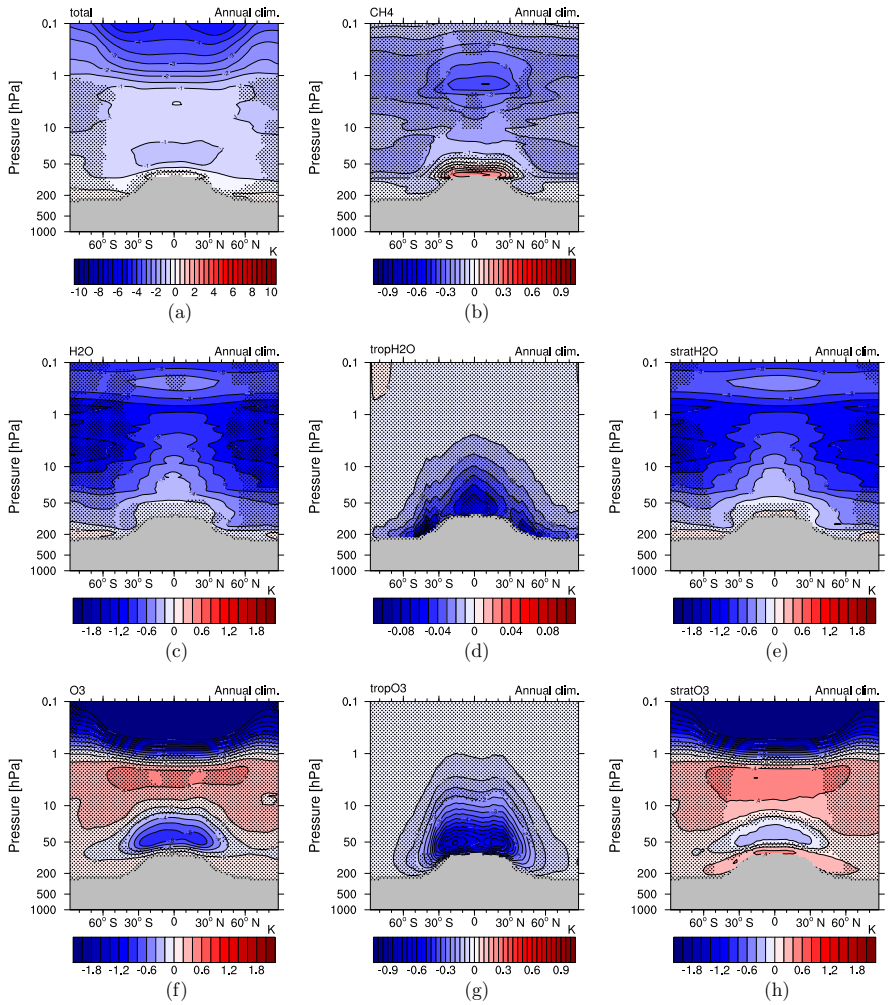

Figure S11. Stratospheric temperature adjustment radiatively induced by individual species changes in simulation S2 MLO (2×methane (CH_4)): (a) CH_4, H_2O and O_3 combined, (b) CH_4, (c) H_2O, (d) tropospheric H_2O only, (e) stratospheric H_2O only (SWV), (f) O_3, (g) tropospheric O_3 only and (h) stratospheric O_3 only. Note the different colour bars in panels (a), (b), (d) and (g).

$\Delta T_{addst}(S2^* - REF^*)_{MLO} - \Delta T_{addst}(S2^* - REF^*)_{fSST}$

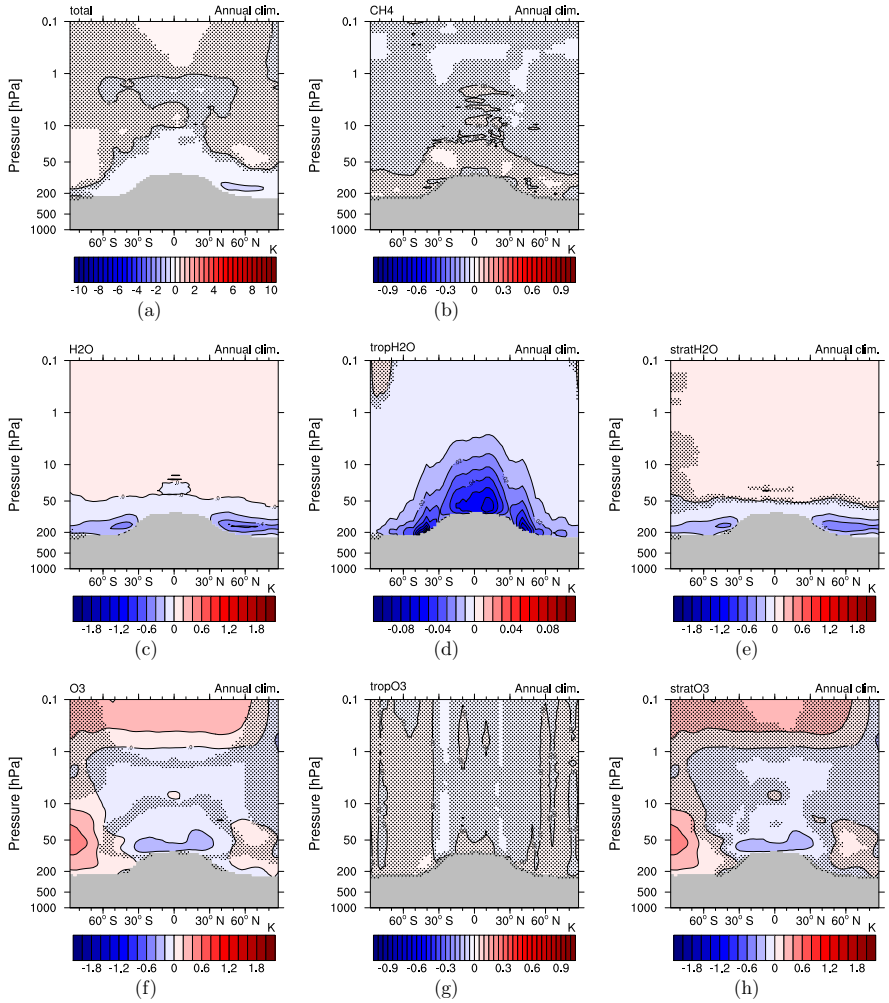

Figure S12. Difference between stratospheric temperature adjustment in simulations S2 MLO and S2 fSST ($2\times CH_4$) radiatively induced by individual species changes: (a) CH_4, H_2O and O_3 combined, (b) CH_4, (c) H_2O, (d) tropospheric H_2O only, (e) stratospheric H_2O only (SWV), (f) O_3, (g) tropospheric O_3 only and (h) stratospheric O_3 only. Note the different colour bars in panels (a), (b), (d) and (g).

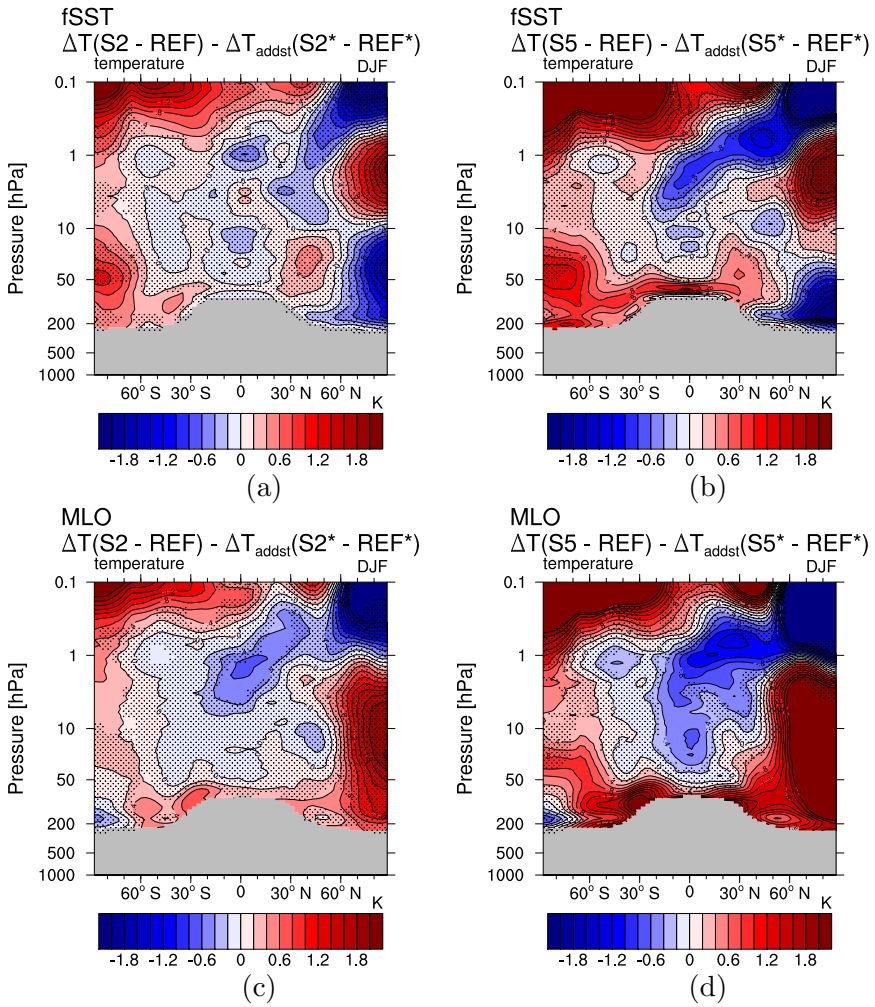

Figure S13. Dynamical temperature response effect for season DJF of the simulations (a) S2 fSST, (b) S5 fSST, (c) S2 MLO, (d) S5 MLO. The dynamical effect is calculated as the difference between the temperature response in the regular simulations (ΔT(SX-REF) with X either 2 or 5) and the sum of the individual contributions of CH_4, H_2O and O_3 to the adjusted stratospheric temperatures (ΔT_{addst}(SX*-REF*) with X either 2 or 5).

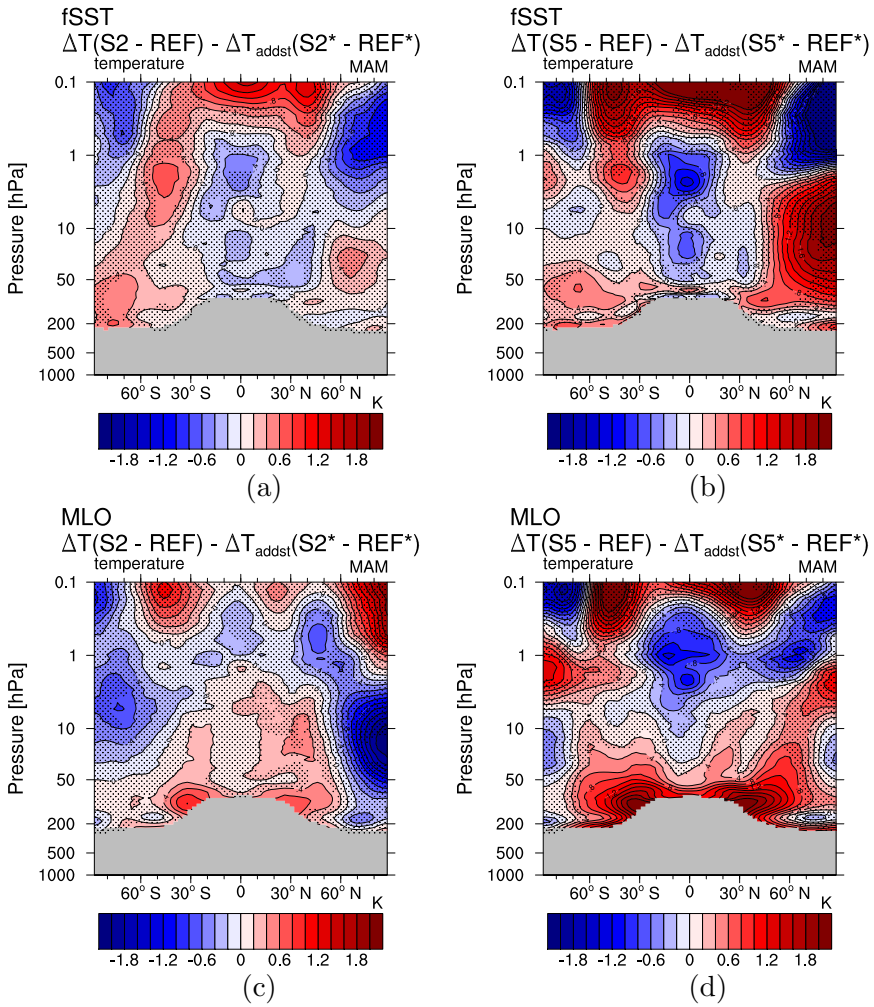

Figure S14. Dynamical temperature response effect for season MAM of the simulations (a) S2 fSST, (b) S5 fSST, (c) S2 MLO, (d) S5 MLO. The dynamical effect is calculated as the difference between the temperature response in the regular simulations (ΔT(SX-REF) with X either 2 or 5) and the sum of the individual contributions of CH_4, H_2O and O_3 to the adjusted stratospheric temperatures (ΔT_{addst}(SX*-REF*) with X either 2 or 5).

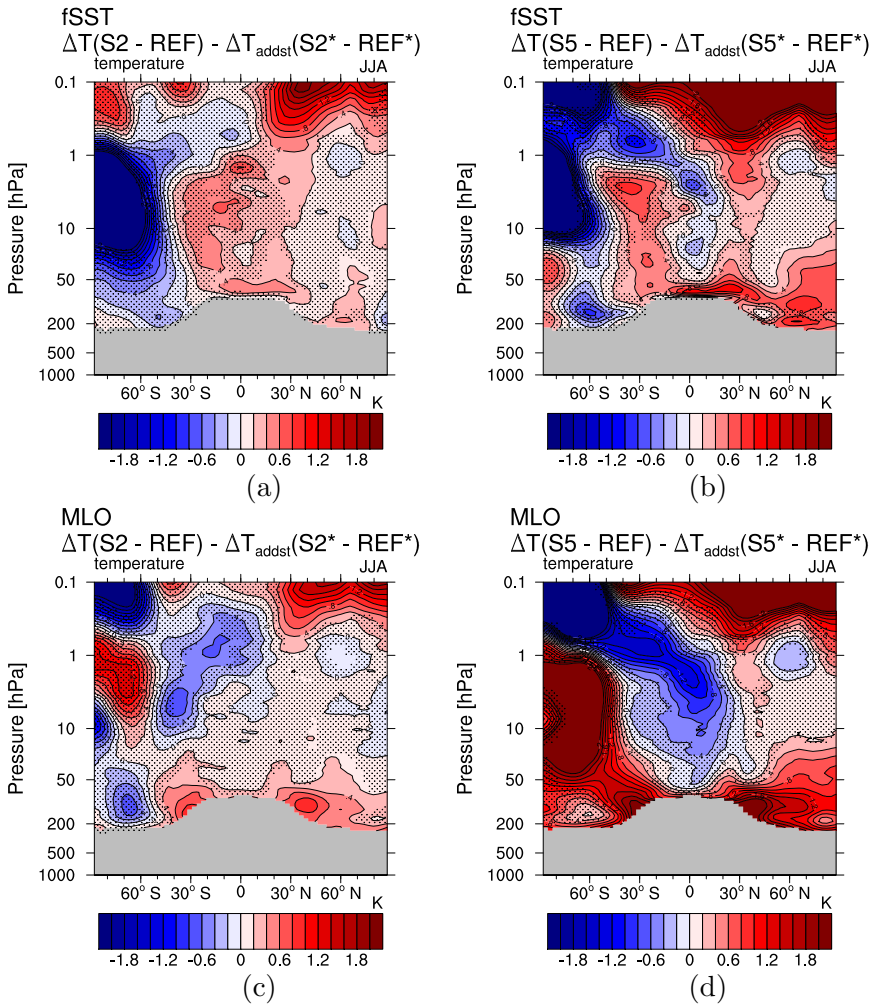

Figure S15. Dynamical temperature response effect for season JJA of the simulations (a) S2 fSST, (b) S5 fSST, (c) S2 MLO, (d) S5 MLO. The dynamical effect is calculated as the difference between the temperature response in the regular simulations (ΔT(SX-REF) with X either 2 or 5) and the sum of the individual contributions of CH_4, H_2O and O_3 to the adjusted stratospheric temperatures (ΔT_{addst}(SX*-REF*) with X either 2 or 5).

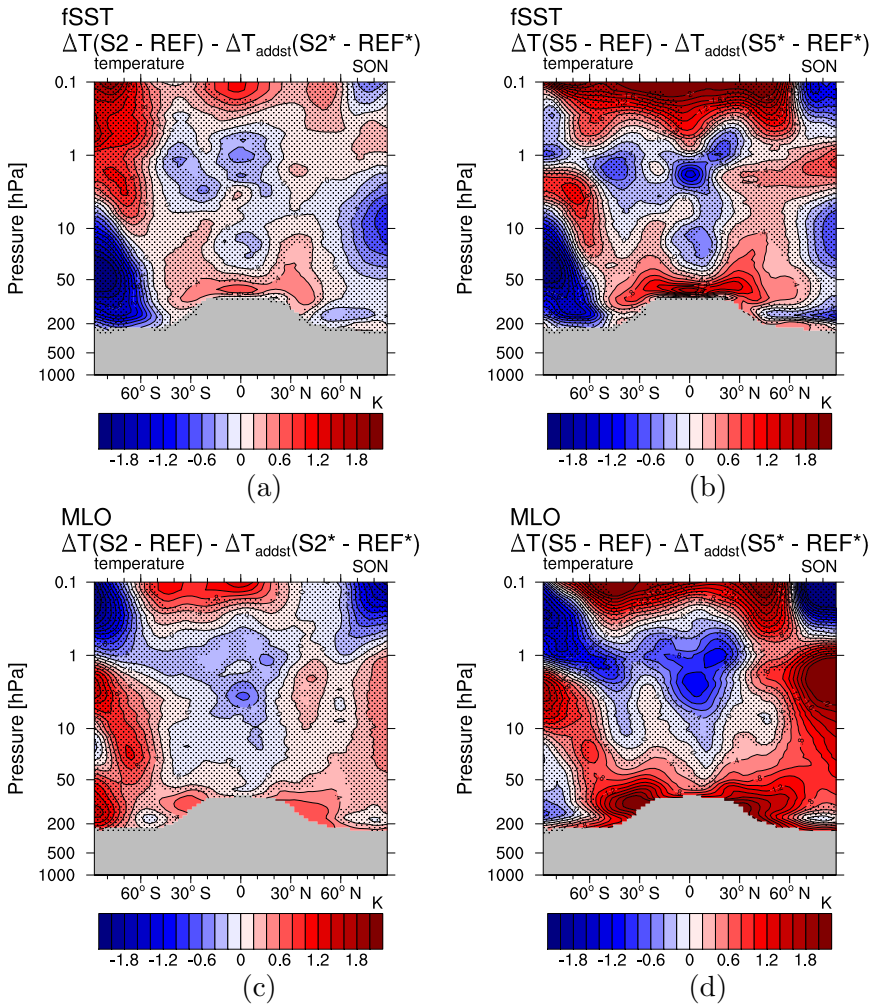

Figure S16. Dynamical temperature response effect for season SON of the simulations (a) S2 fSST, (b) S5 fSST, (c) S2 MLO, (d) S5 MLO. The dynamical effect is calculated as the difference between the temperature response in the regular simulations (ΔT(SX-REF) with X either 2 or 5) and the sum of the individual contributions of CH_4, H_2O and O_3 to the adjusted stratospheric temperatures (ΔT_{addst}(SX*-REF*) with X either 2 or 5).

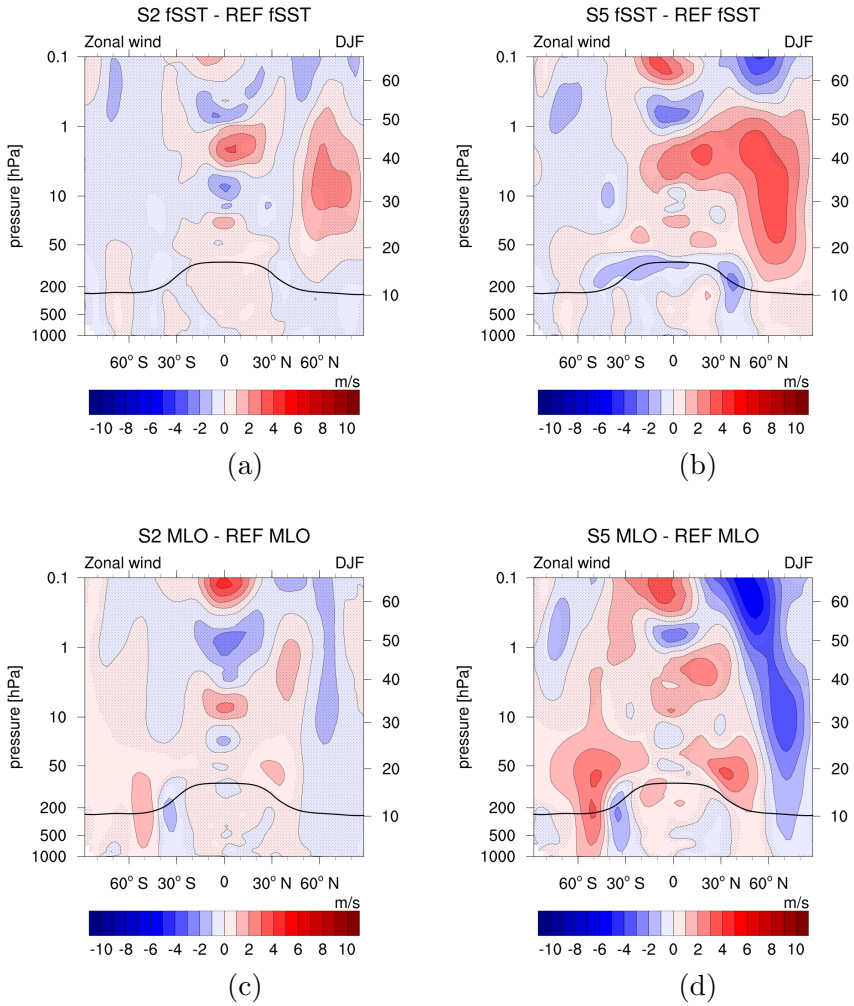

Figure S17. Absolute differences of zonal wind for season DJF of the sensitivity simulations (a) S2 fSST, (b) S5 fSST, (c) S2 MLO, (d) S5 MLO and their respective reference in m s^{-1}. Non-stippled areas are significant on the 95 % confidence level according to a two sided Welch's test. The solid black line indicates the climatological tropopause height of REF MLO.

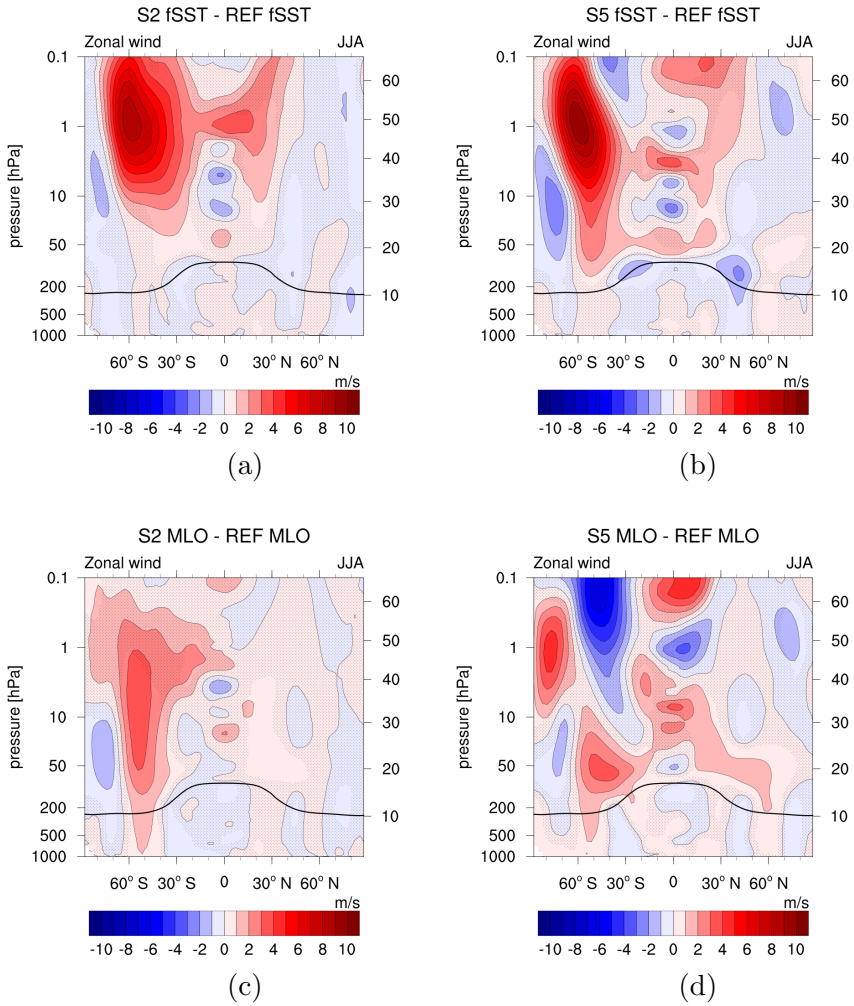

Figure S18. Absolute differences of zonal wind for season JJA of the sensitivity simulations (a) S2 fSST, (b) S5 fSST, (c) S2 MLO, (d) S5 MLO and their respective reference in m s^{-1}. Non-stippled areas are significant on the 95 % confidence level according to a two sided Welch's test. The solid black line indicates the climatological tropopause height of REF MLO.

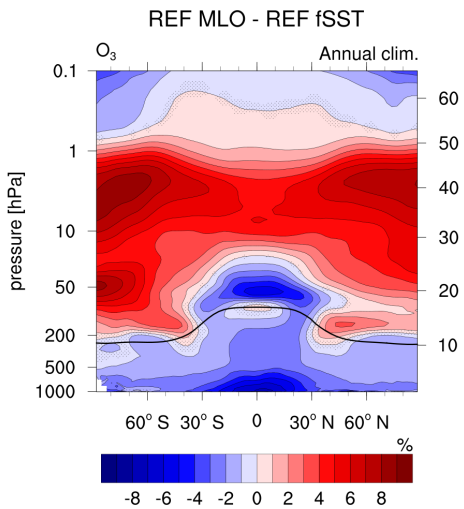

Figure S19. Relative differences of the annual zonal mean O_3 mixing ratio of REF MLO with respect to REF fSST in %. Non-stippled areas are significant on a 95 % confidence level according to a two sided Welch's test. The solid black line indicates the climatological tropopause height of the REF MLO.

Table S1. List of reactions, for which reaction coefficients changed from MESSy version 2.52 (fSST) to MESSy version 2.54.0 (MLO) in submodel Module Efficiently Calculating the Chemistry of the Atmosphere (MECCA; Sander et al. (2011a)).

Reaction	Reference for Reaction Rate Coefficient	
	fSST	MLO
$HO_2 + HO_2 \rightarrow H_2O_2 + O_2$	Christensen et al. (2002), Kircher and Sander (1984)	Burkholder et al. (2015)
$NO_3 + NO_2 \rightarrow N_2O_5$ $N_2O_5 \rightarrow NO_3 + NO_2$	Sander et al. (2011b)	Burkholder et al. (2015)
$NO_2 + HO_2 \rightarrow HNO_4$ $HNO_4 \rightarrow NO_2 + HO_2$	Sander et al. (2011b)	Burkholder et al. (2015)
$ClO + ClO \rightarrow Cl_2O_2$ $Cl_2O_2 \rightarrow ClO + ClO$	Atkinson et al. (2007) Atkinson et al. (2007), Sander et al. (2011b)	Burkholder et al. (2015)
$N_2O + O(^1D) \rightarrow$ 1.0 LossO3O + 1. LossO3 + 2 NO $N_2O + O(^1D) \rightarrow$ 1.0 LossO3O + 1. LossO3 + $N_2 + O_2$	Sander et al. (2011b)	Burkholder et al. (2015)
$ClO + CH_3O_2 \rightarrow$ 1.0 LossO3Cl + 1. LossO3 + HO_2 + Cl + HCHO	Sander et al. (2011b)	Burkholder et al. (2015)
$CH_3Cl + OH \rightarrow$ 1.0 ProdLCl + LCARBON + H_2O + Cl	Sander et al. (2011b)	Burkholder et al. (2015)
$CH_3CCl_3 + O(^1D) \rightarrow$ 3.0 ProdLCl + 1.0 LossO3Cl + 1.LossO3 + 2 LCARBON + OH + 3 Cl	extrapolation from reactions with CH_3CF_3, CH_3CClF_2 and CH_3CCl_2F from Sander et al. (2006)	Burkholder et al. (2015)
$CH_3Br + OH \rightarrow$ 1.0 ProdLBr + LCARBON + H_2O + Br	Sander et al. (2011b)	Burkholder et al. (2015)
$CHBr_3 + OH \rightarrow$ 3.0 ProdSBr + LCARBON + H_2O + 3 Br	Sander et al. (2011b)	Burkholder et al. (2015)
$CH_2ClBr + OH \rightarrow$ 1.0 ProdSBr + LCARBON + LCHLORINE + H_2O + Br	Sander et al. (2011b)	Burkholder et al. (2015)
$HNO_3 + OH \rightarrow$ 1. ProdO3 + H_2O + NO_3	Sander et al. (2011b)	Dulitz et al. (2018)

References

Atkinson, R., Baulch, D. L., Cox, R. A., Crowley, J. N., Hampson, R. F., Hynes, R. G., Jenkin, M. E., Rossi, M. J., and Troe, J.: Evaluated kinetic and photochemical data for atmospheric chemistry: Volume III – gas phase reactions of inorganic halogens, Atmos. Chem. and Phys., 7, 981–1191, https://doi.org/10.5194/acp-7-981-2007, https://www.atmos-chem-phys.net/7/981/2007/, 2007.

Burkholder, J. B., Sander, S. P., Abbatt, J. P. D., Barker, J. R., Huie, R. E., Kolb, C. E., Kurylo, M. J., Orkin, V. L., Wilmouth, D. M., and Wine, P. H.: Chemical Kinetics and Photochemical Data for Use in Atmospheric Studies, Evaluation No. 18, JPL Publication 15-10, Jet Propulsion Laboratory, http://jpldataeval.jpl.nasa.gov/, 2015.

Christensen, L. E., Okumura, M., Sander, S. P., Salawitch, R. J., Toon, G. C., Sen, B., Blavier, J.-F., and Jucks, K. W.: Kinetics of HO_2 + $HO_2 \rightarrow H_2O_2$ + O_2: Implications for Stratospheric H_2O_2, Geophys. Res. Lett., 29, 13–1–13–4, https://doi.org/10.1029/2001GL014525, https://doi.org/10.1029/2001GL014525, 2002.

Dulitz, K., Amedro, D., Dillon, T. J., Pozzer, A., and Crowley, J. N.: Temperature-(208–318 K) and pressure-(18–696 Torr) dependent rate coefficients for the reaction between OH and HNO_3, Atmos. Chem. Phys., 18, 2381–2394, https://doi.org/10.5194/acp-18-2381-2018, https://doi.org/10.5194/acp-18-2381-2018, 2018.

Kircher, C. C. and Sander, S. P.: Kinetics and mechanism of HO_2 and DO_2 disproportionations, J. Phys. Chem., 88, 2082–2091, https://doi.org/10.1021/j150654a029, https://doi.org/10.1021/j150654a029, 1984.

Rayner, N. A., Parker, D. E., Horton, E. B., Folland, C. K., Alexander, L. V., Rowell, D. P., Kent, E. C., and Kaplan, A.: Global analyses of sea surface temperature, sea ice, and night marine air temperature since the late nineteenth century, J. Geophys. Res. Atmos., 108, https://doi.org/10.1029/2002JD002670, 4407, 2003.

Sander, R., Baumgaertner, A., Gromov, S., Harder, H., Jöckel, P., Kerkweg, A., Kubistin, D., Regelin, E., Riede, H., Sandu, A., Taraborrelli, D., Tost, H., and Xie, Z.-Q.: The atmospheric chemistry box model CAABA/MECCA-3.0, Geosci. Model Dev., 4, 373–380, https://doi.org/10.5194/gmd-4-373-2011, 2011a.

Sander, S. P., Friedl, R. R., Golden, D. M., Kurylo, M. J., Moortgat, G. K., Keller-Rudek, H., Wine, P. H., Ravinshankara, A. R., Kolb, C. E., Molina, M. J., Finlayson-Pitts, B. J., Huie, R. E., and Orkin, V. L.: Chemical Kinetics and Photochemical Data for Use in Atmospheric Studies, Evaluation No. 15, JPL Publication 06-2, Jet Propulsion Laboratory, http://jpldataeval.jpl.nasa.gov, 2006.

Sander, S. P., Abbatt, J., Barker, J. R., Burkholder, J. B., Friedl, R. R., Golden, D. M., Huie, R. E., Kolb, C. E., Kurylo, M. J., Moortgat, G. K., Orkin, V. L., and Wine, P. H.: Chemical Kinetics and Photochemical Data for Use in Atmospheric Studies, Evaluation No. 17, JPL Publication 10-6, Jet Propulsion Laboratory, https://doi.org/10.1002/kin.550171010, http://jpldataeval.jpl.nasa.gov/, 2011b.